Supporting Information

Novel hybrid capacitive deionization constructed by redox-active covalent organic framework and its derived porous carbon for highly efficient desalination

Yuquan Li,[a] Zibiao Ding,[a] Xinlu Zhang,[a] Jingliang Li,[b] Xinjuan Liu,[c] Ting Lu,[a] Yefeng Yao,[a] Likun Pan*[a]

[a] Shanghai Key Laboratory of Magnetic Resonance,

School of Physics and Materials Science, East China Normal University, Shanghai 200062, China

*Corresponding author. Tel.: +8621 62234132; fax: +8621 62234321;

E-mail address: lkpan@phy.ecnu.edu.cn

[b] Siyuan Laboratory, Guangdong Provincial Engineering Technology Research Center of Vacuum Coating Technologies and New Energy Materials, Department of Physics, Jinan University, Guangzhou, Guangdong 510632, China.

[c] Institute of Optoelectronic Materials and Devices, College of Optical and Electronic Technology, China Jiliang University, Hangzhou, 310018, China.

The mass ratio of active materials on anode and cathode in HCDI

The mass ratio of active materials on anode and cathode in asymmetric HCDI is determined by the ratio of their specific capacities obtained from galvanostatic charging/discharging tests at 0.1 A g^{-1}. To make full use of high capacity of DAAQ-TFP-COF, 0.9 V was applied on DAAQ-TFP-COF cathode (as exhibited in Figure 7c and Figure 9c). Meanwhile, to suppress water splitting, the voltage on carbon anode is set at 0.6 V (conventional symmetric CDI is operated at 1.2 V cell voltage). The specific capacities (mAh g^{-1}) of DAAQ-TFP-COF cathode and NPC-700 anode were calculated based on following Eq S1:

$$specific\ capacity = \frac{C \times V}{3.6} \qquad (S1)$$

where C is specific capacitance (F g^{-1}) and V (V) is the applied voltage on the electrode. The specific capacities of DAAQ-TFP-COF and NPC-700 are 42.7 and 21.6 mAh g^{-1}, respectively. Considering the ratio of their specific capacities is approximately 2: 1, the mass ratio of active materials on anode and cathode is fixed at 2: 1.

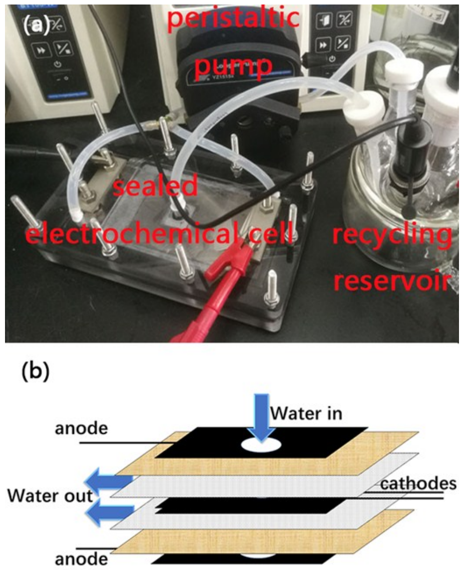

Figure S1 (a) The digital photograph and (b) construction of CDI cell.

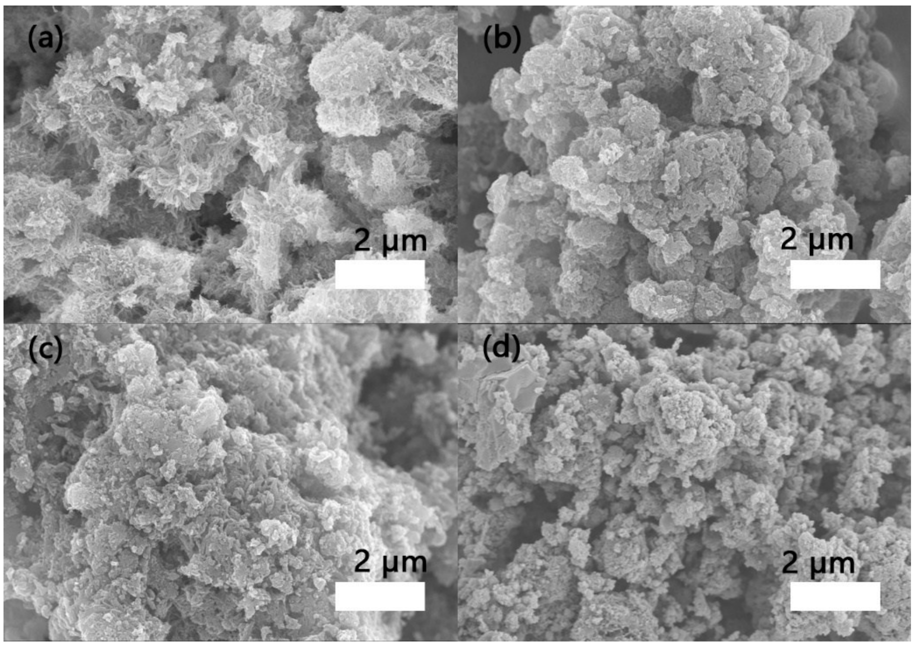

Figure S2 FESEM images of (a) DAAQ-TFP-COF, (b) NPC-500, (c) NPC-700 and (d) NPC-900 at low magnification.

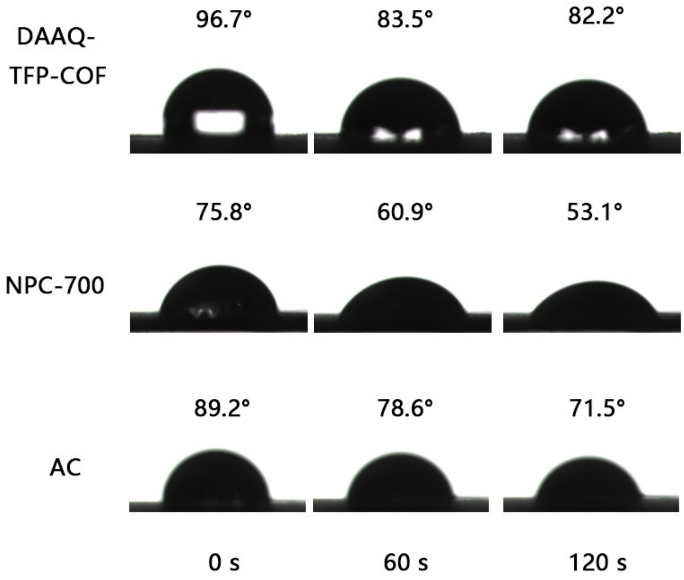

Figure S3 Optical micrographs of water contact angles on DAAQ-TFP-COF, NPC-700 and AC electrodes at different time.

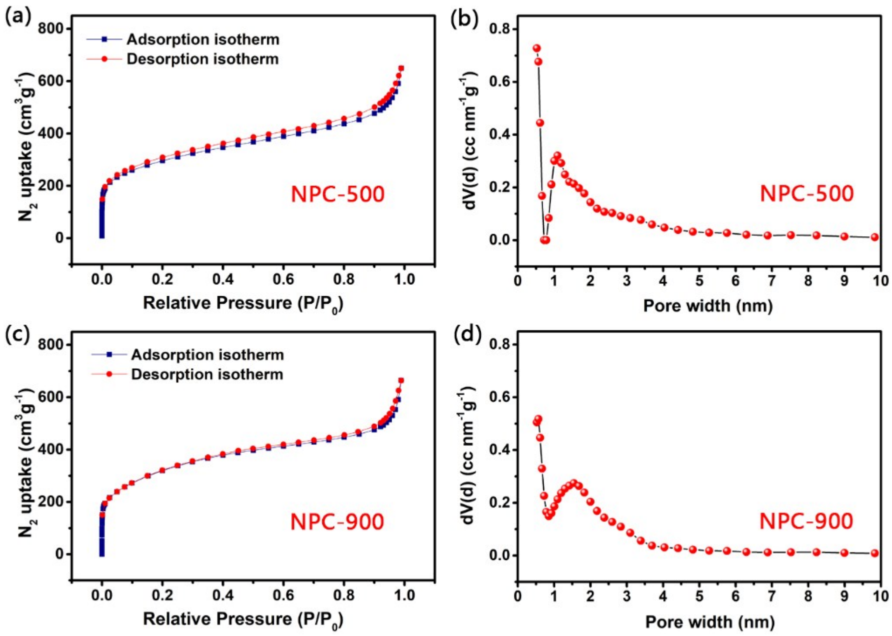

Figure S4 (a) Nitrogen adsorption–desorption isotherms and NLDFT pore size distributions of NPC-500 (a and b) and NPC-900 (c and d).

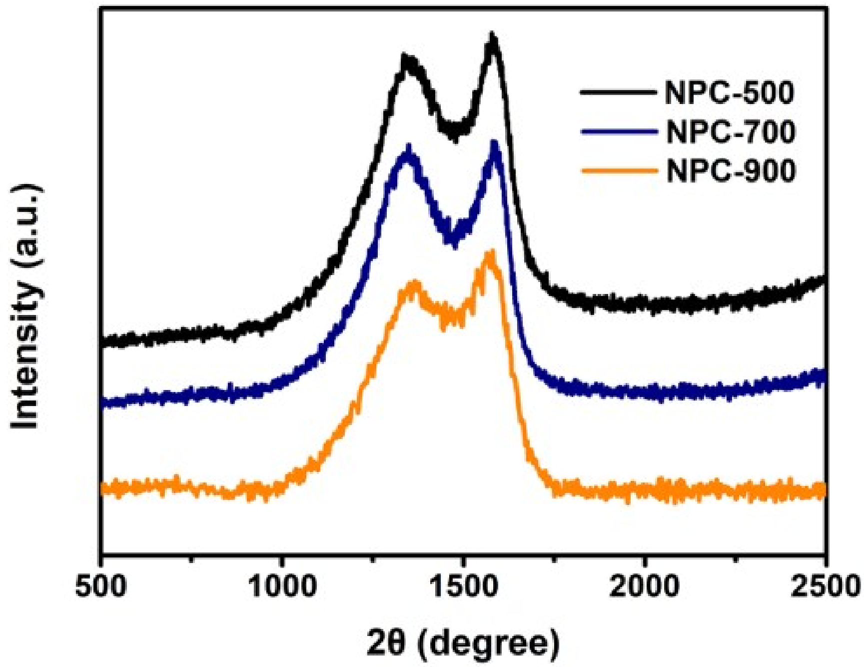

Figure S5 Raman spectra of NPCs.

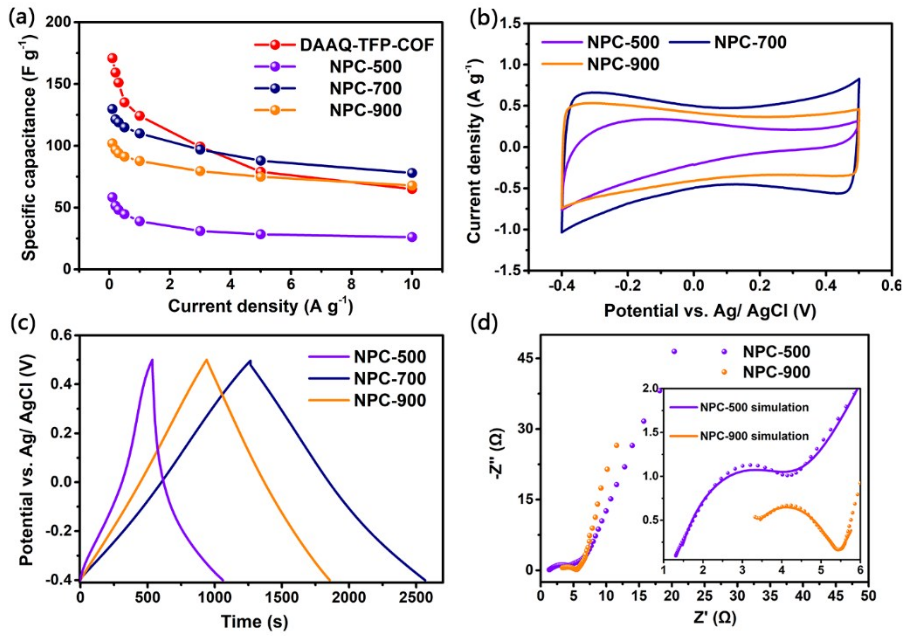

Figure S6 (a) Specific capacitances of DAAQ-TFP-COF and NPCs at different current densities. (b) CV curves of NPCs at 5 mV s^{-1}. (c) GCD curves of NPCs at 0.1 A g^{-1}. (d) Nyquist plots of NPC-500 and NPC-900. Inset of (d) shows the magnified plots in high-frequency region. All the curves were obtained in 1 M NaCl solution.

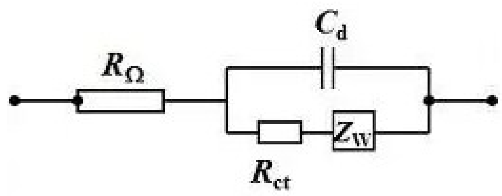

Figure S7 Equivalent circuit model used for fitting Nyquist plots.

Table S1 Specific capacitances at 0.1 A g^{-1} and R_{ct} values of the samples.

Samples	Specific capacitance (F g^{-1})	R_{ct} (Ω)
DAAQ-TFP-COF	170.9	1.26
NPC-500	58.3	3.27
NPC-700	129.8	1.08
NPC-900	101.9	2.58

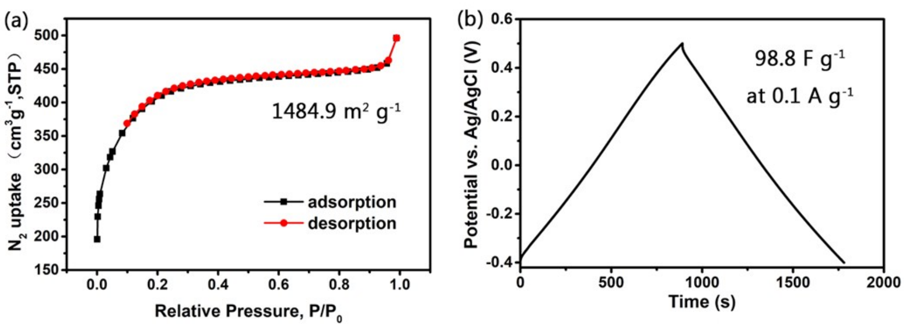

Figure S8 (a) Nitrogen adsorption-desorption isotherm and (b) galvanostatic charge-discharge curve of activated carbon at a current density of 0.1 A g^{-1} tested in 1 M NaCl solution.

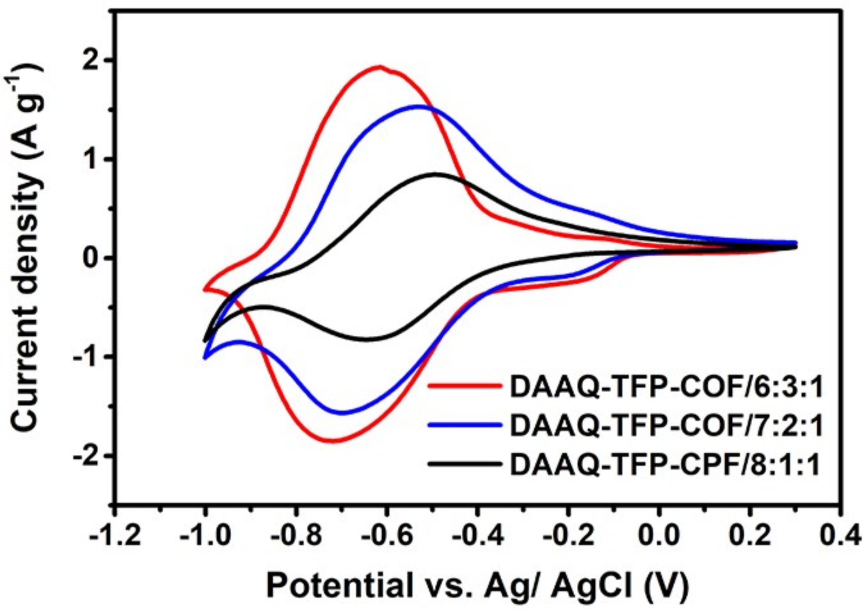

Figure S9 CV plots of DAAQ-TFP-COF electrode with different carbon black additions in 1 M NaCl solutions at 5 mV s^{-1} scan rate.

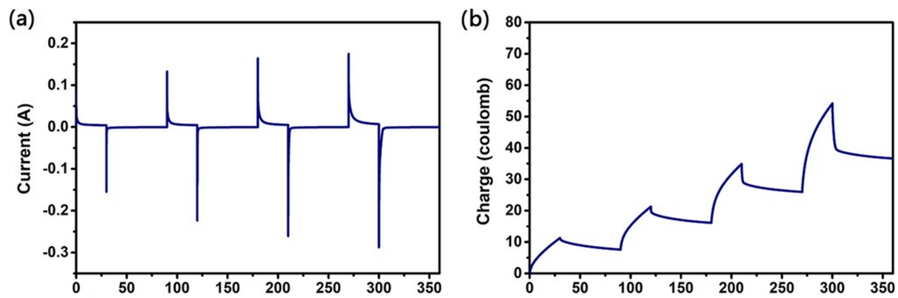

Figure S10 Current and integral charge plots of NPC//DAAQ-TFP-COF HCDI tested at different cell voltages with an initial concentration of 500 ppm.

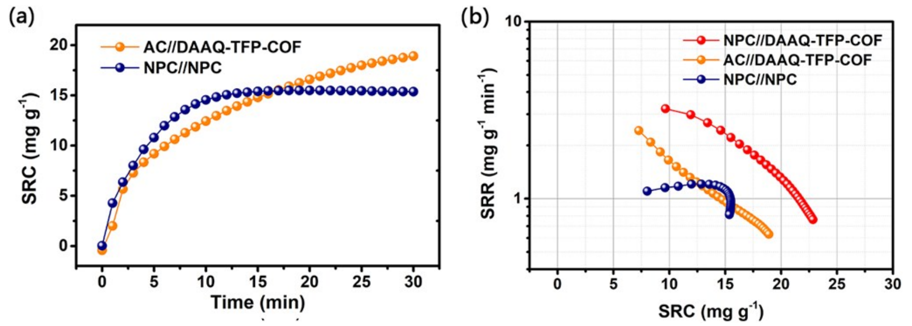

Figure S11 (a) Desalination performances of AC//DAAQ-TFP-COF HCDI cell at 1.6 V cell voltage and symmetric NPC-700//NPC-700 CDI cell in 500 ppm NaCl solution. (b) Comparison of Ragone plots (SRR vs SRC) of different cell configurations.

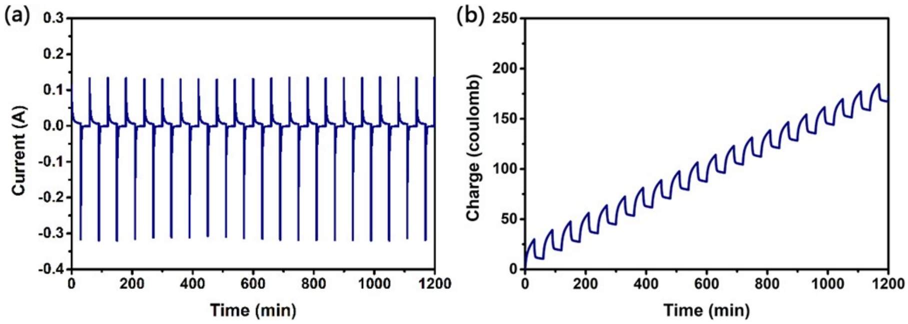

Figure S12 Current and integral charge plots in the cycling test.

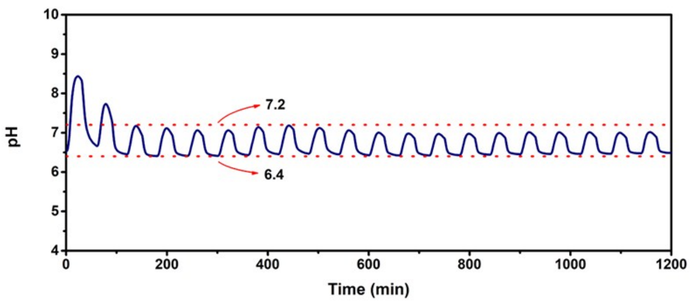

Figure S13 pH fluctuation in the cycling test.

Table S2 Comparison of desalination performance between various faradaic electrode materials reported for CDI application.

Electrode material	SRC	Initial NaCl	Type	Ref.

	(mg g^{-1})	concentration (mg L^{-1})		
MnO_2-multiwall carbon nanotube (CNT)*	6.65	87	pseudocap.	1
BCN nanosheets*	13.6	500	pseudocap.	2
MXene*	13	292	pseudocap.	3
$Mo_{1.33}C$-MXene*	15	35064	pseudocap.	4
MoS_2 nanosheets*	8.8	23376	pseudocap.	5
MoS_2-CNT*	25	29220	pseudocap.	6
g-Al_2O_3-CNT //SiO_2-CNT	6.5	2000	pseudocap.	7
CNT-V_2O_5//AC	25	53064	pseudocap.	8
hydrated vanadyl phosphate//AC	24.3	5844	battery	9
NiHCF//AC	34	29220	battery	10
$Na_4Mn_9O_{18}$//AC	31.2	2922	battery	11
$Na_2FeP_2O_7$//AC	30.2	5844	battery	12
DAAQ-TFP-COF//NPC-700	22.8	500	pseudocap.	This work
	29.6	6000		

*Using symmetric cell construction.

1. B. Chen, Y. Wang, Z. Chang, X. Wang, M. Li, X. Liu, L. Zhang and Y. Wu, *RSC Adv.*, 2016, **6**, 6730-6736.
2. S. Wang, G. Wang, T. Wu, Y. Zhang, F. Zhan, Y. Wang, J. Wang, Y. Fu and J. Qiu, *J. Mater. Chem. A*, 2018, **6**, 14644-14650.
3. P. Srimuk, F. Kaasik, B. Krüner, A. Tolosa, S. Fleischmann, N. Jäckel, M. C. Tekeli, M. Aslan, M. E. Suss and V. Presser, *J. Mater. Chem. A*, 2016, **4**, 18265-18271.

4. P. Srimuk, J. Halim, J. Lee, Q. Tao, J. Rosen and V. Presser, *ACS Sustain. Chem. Eng.*, 2018, **6**, 3739-3747.
5. F. Xing, T. Li, J. Li, H. Zhu, N. Wang and X. Cao, *Nano Energy*, 2017, **31**, 590-595.
6. P. Srimuk, J. Lee, S. Fleischmann, S. Choudhury, N. Jäckel, M. Zeiger, C. Kim, M. Aslan and V. Presser, *J. Mater. Chem. A*, 2017, **5**, 15640-15649.
7. C. Santos, J. J. Lado, E. García-Quismondo, I. V. Rodríguez, J. Palma, M. A. Anderson and J. J. Vilatela, *J. Mater. Chem. A*, 2018, **6**, 10898-10908.
8. J. Lee, P. Srimuk, K. Aristizabal, C. Kim, S. Choudhury, Y. C. Nah, F. Mücklich and V. Presser, *ChemSusChem*, 2017, **10**, 3611-3623.
9. J. Lee, P. Srimuk, R. Zwingelstein, R. L. Zornitta, J. Choi, C. Kim and V. Presser, *J. Mater. Chem. A*, 2019.
10. S. Porada, A. Shrivastava, P. Bukowska, P. Biesheuvel and K. C. Smith, *Electrochim. Acta*, 2017, **255**, 369-378.
11. J. Lee, S. Kim, C. Kim and J. Yoon, *Energy Environ. Sci.*, 2014, **7**, 3683-3689.
12. S. Kim, J. Lee, C. Kim and J. Yoon, *Electrochim. Acta*, 2016, **203**, 265-271.